Estimating the Velocity Profile and Acoustical Quantities of a Harmonically Vibrating Loudspeaker Membrane from On-Axis Pressure Data*

RONALD M. AARTS,[1,2] *AES Fellow,* **AND AUGUSTUS J. E. M. JANSSEN**[1]
(ronald.m.aarts@philips.com) (a.j.e.m.janssen@ieee.org)

[1]*Philips Research Laboratories, 5656AE Eindhoven, The Netherlands*
[2]*Eindhoven University of Technology, Department of Electrical Engineering, 5600 MB Eindhoven, The Netherlands*

Formulas are presented for the acoustical quantities of a harmonically excited resilient, flat circular loudspeaker in an infinite baffle, which are the sound pressure both on axis and far field, the directivity, and the total radiated power. These quantities are obtained by expanding the velocity distribution in terms of orthogonal polynomials. For rigid and nonrigid radiators this yields explicit series expressions for both the on-axis and the far-field pressure. In the reverse direction, a method of estimating velocity distributions from (measured) on-axis pressures by matching in terms of expansion coefficients is described. Together with the forward far-field computation scheme, this yields a method for the assessment of loudspeakers in the far field and of the total radiated power from (relatively near-field) on-axis data (generalized Keele scheme).

0 INTRODUCTION

In this paper an analytic method developed in [1], [2] for the calculation of acoustical quantities such as the sound pressure both on axis and far field, the directivity, and the total radiated power is presented to the audio engineering community. This method is based on the analytical results as developed in the diffraction theory of optical aberrations by Nijboer [3] and Zernike and Nijboer [4]; see also [5], [6]. Using this approach, many of the analytic results in Greenspan [7], such as those for the sound pressure on axis, the total radiated power, and the results in text books [8] regarding far-field expressions and directivity can be presented and extended in a systematic fashion. This is worked out in [1] for on-axis pressure and far-field expressions for arbitrary velocity distributions on flat piston radiators. The mathematical foundation of these methods related to directivity and the total radiated power is discussed in [2]. An arbitrary velocity distribution can be developed efficiently as a series in Zernike polynomials. Using near-field pressure measurements on axis the coefficients of these polynomials can be estimated. With these estimated coefficients the acoustical quantities mentioned can be estimated as well. An immediate application is to predict far-field sound pressure data from near-field pressure data measured without using an anechoic chamber (generalized Keele scheme [1], [9]).

The radiated pressure is given in integral form by the Rayleigh integral [8], [10] as

$$p(\boldsymbol{r},t)=\frac{\mathrm{i}\rho_0 ck}{2\pi}\mathrm{e}^{\mathrm{i}\omega t}\int_S v(\boldsymbol{r}_\mathrm{s})\frac{\mathrm{e}^{-\mathrm{i}kr'}}{r'}\,\mathrm{d}S \tag{1}$$

where ρ_0 is the density of the medium, c is the speed of sound in the medium, $k=\omega/c$ is the wavenumber, and ω is the radian frequency of the harmonically vibrating surface S. Furthermore t is time, $\boldsymbol{r}$ is a field point, $\boldsymbol{r}_\mathrm{s}$ is a point on the surface S, $r'=|\boldsymbol{r}-\boldsymbol{r}_\mathrm{s}|$ is the distance between $\boldsymbol{r}$ and $\boldsymbol{r}_\mathrm{s}$, and $v(\boldsymbol{r}_\mathrm{s})$ is the normal component of a (not necessarily uniform) velocity profile on the surface S. The time variable t in $p(\boldsymbol{r}, t)$ and the harmonic factor $\exp(\mathrm{i}\omega t)$ in front of the integral in Eq. (1) will be omitted in the sequel. For transparency of exposition, the surface S is assumed [1], [2] to be a disk of radius a, $|\boldsymbol{r}_\mathrm{s}|=r_\mathrm{s}\le a$, with average velocity V_s. In [1] a generalization to the case of dome-shaped radiator surfaces S is made. In [11] a generalization for a loudspeaker modeled as a resilient spherical cap on a rigid sphere is presented. See Fig. 1 for the geometry

*Presented at the 126th Convention of the Audio Engineering Society, Munich, Germany, 2009 May 7–10; revised 2009 October 26.

and notation used in the case of a flat piston. The volume velocity V at the piston is

$$V = \int_S v(\boldsymbol{r}_s)\,\mathrm{d}S = V_s\,\pi a^2. \tag{2}$$

Frankort [12] has shown that loudspeaker cones vibrate mainly in a radially symmetric fashion. This is certainly not the case for all loudspeakers in general the limitation is further discussed in Section 6, but in this paper our attention is restricted to radially symmetric velocity distributions v, which are denoted by $v(\sigma)$, $0 \le \sigma \le a$. Define the Zernike terms [3], [4],

$$R^0_{2n}(\rho) = P_n(2\rho^2 - 1), \qquad 0 \le \rho \le 1 \tag{3}$$

where P_n are the Legendre polynomials [13]. By completeness and orthogonality [see Eq. (9)] the velocity profile $v(\sigma)$ admits the representation

$$v(\sigma) = V_s \sum_{n=0}^{\infty} u_n R^0_{2n}(\sigma/a), \qquad 0 \le \sigma \le a \tag{4}$$

in which u_n are scalar coefficients [see Eq. (5)]. In [1] analytical results are presented for the on-axis and far-field pressure $p(\boldsymbol{x})$ in Eq. (1) related to the coefficients u_n and polynomials R^0_{2n} occurring in the expansion in Eq. (4).

By orthogonality of the terms $R^0_{2n}(\rho)$ the coefficients u_n in Eq. (4) can be found in integral form as

$$u_n = \frac{2(2n+1)}{V_s} \int_0^1 R^0_{2n}(\rho) v(a\rho) \rho\,\mathrm{d}\rho, \qquad n = 0, 1, \ldots. \tag{5}$$

In particular, $u_0 = 1$. There are an impressive number of cases where one can explicitly find the u_n in Eq. (5). These include the rigid piston ($\ell = 0$), the simply supported radiator ($\ell = 1$), and the higher order clamped radiators ($\ell \ge 2$) with the velocity profile of Stenzel [14], given in Greenspan's notation [7] as

$$v^{(\ell)}(\sigma) = (\ell + 1)\,V_s \left[1 - (\sigma/a)^2\right]^{\ell} H(a - \sigma), \qquad \ell = 0, 1, \ldots \tag{6}$$

and the Gaussian velocity profile

$$v(\sigma;\, \alpha) = \frac{\alpha V_s}{1 - \mathrm{e}^{-\alpha}} \mathrm{e}^{-\alpha(\sigma/a)^2} H(a - \sigma) \tag{7}$$

where $H(x)$ is the Heaviside function. $H(x) = 0$, 1/2, or 1 according to whether x is negative, zero, or positive. Hence the velocity profiles in Eqs. (6) and (7) vanish for $\sigma > a$. This is illustrated in Fig. 2, where various profiles are plotted.

The relevance of the Zernike terms R^0_{2n} for the purposes of the present paper is the existence of closed-form formulas. For instance, the radiators in Eq. (6) give rise to an on-axis pressure expansion in the form of a series of $n + 1$ terms $u_\ell j_\ell(kr_-)h^{(2)}_\ell(kr_+)$, with $r_\pm$ argument values directly related to the axial position $(0, 0, r)$, while the far-field pressure expansion is a similar series involving terms $u_\ell J_{2\ell+1}(ka\sin\theta)/(ka\sin\theta)$. In [2] it is shown how the acoustic power P and the directivity D are computed from the coefficients u_ℓ. In the reverse direction the forward computation schemes for the on-axis and far-field pressures is complemented in [1] by an inverse method with potential use in far-field loudspeaker assessment. Here one estimates the expansion coefficients u_n of a velocity profile v by matching against a measured on-axis pressure data set, and then one predicts the far-field sound radiation using the far-field forward formula.

1 PAPER OUTLINE

In Section 2 the definition and the basic properties of the Zernike polynomials are given, and some of the expansion results that are relevant for this paper are presented. Furthermore the Hankel transform of the Zernike polynomials is presented in closed form. The latter result is of importance both for the forward computation scheme for the far field and for establishing results on the radiated power.

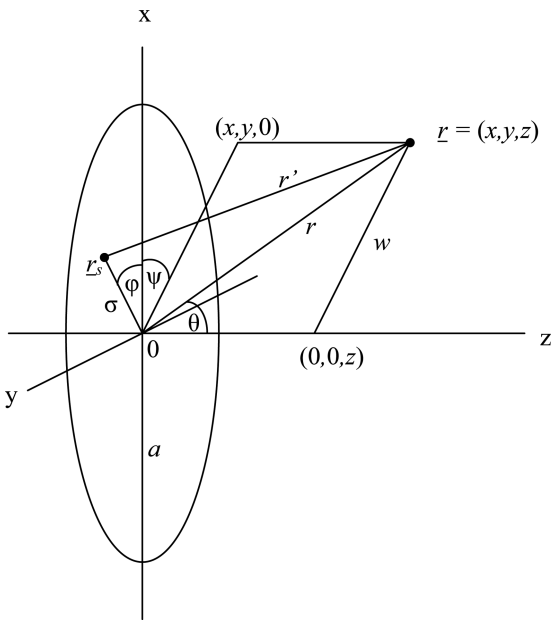

$\boldsymbol{r}_s = (x_s, y_s, 0) = (\sigma\cos\varphi, \sigma\sin\varphi, 0)$
$\boldsymbol{r} = (x, y, z) = (r\sin\theta\cos\psi, r\sin\theta\sin\psi, r\cos\theta)$
$w = r\sin\theta = (x^2 + y^2)^{1/2}$, $z = r\cos\theta$
$r = |\boldsymbol{r}| = (x^2 + y^2 + z^2)^{1/2} = (w^2 + z^2)^{1/2}$
$r' = |\boldsymbol{r} - \boldsymbol{r}_s| = [r^2 + \sigma^2 - 2\sigma w\cos(\psi - \varphi)]^{1/2}$

Fig. 1. Setup and notations.

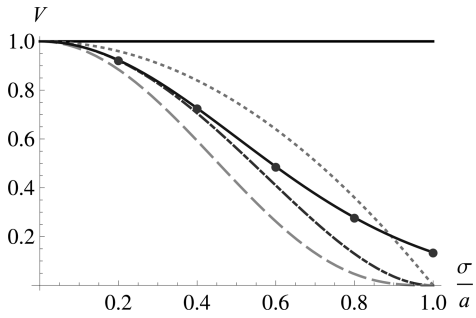

Fig. 2. Normalized velocity profiles V for rigid piston ($\ell = 0$) (——); simply supported radiator ($\ell = 1$) (···); and first two clamped radiators ($\ell = 2$, 3) (–·–; – – –) using Eq. (6); and truncated Gaussian profile ($\alpha = 2$, –•–) using Eq. (7). Normalization is such that $V = 1$ for $\sigma/a = 0$; $V = 0$ for $|\sigma/a| > 1$.

In Section 3 the basic formulas are highlighted and discussed. Thus the closed form involving a spherical Bessel and Hankel function for the on-axis pressure associated with a single Zernike term is presented, with comments on both near-field and far-field behavior and on behavior for low and high frequencies in terms of ka. Also the far-field expression is presented as derived in [1].

In Section 4 the formulas [2] for the total radiated power and directivity are presented and discussed.

In Section 5 the inverse method [1] of estimating the Zernike expansion coefficients of the velocity profile from the on-axis (measured, sampled) pressure data is considered. Together with the forward scheme for computing far-field pressures from Zernike expansions, this yields a loudspeaker assessment method that generalizes a well-known method in audio engineering for estimating the far field of a loudspeaker from near-field on-axis data in the case of a rigid piston (Keele scheme [9]).

In the present paper only a few measurements and simulation results will be shown.

2 THE ZERNIKE TERMS R_{2n}^0

The Zernike terms R_{2n}^0 are polynomials of degree $2n$ given by

$$R_{2n}^0(\sigma/a) = P_n\left[2(\sigma/a)^2-1\right] = \sum_{s=0}^{n}(-1)^s\binom{2n-s}{n}\binom{n}{s}(\sigma/a)^{2n-2s} \quad (8)$$

where P_n is the Legendre polynomial of degree n (see [13, secs. 22.3.8 and 22.5.42]). The first few R_{2n}^0 are given in Table 1, and in Fig. 3 some are plotted as a function of $\rho = \sigma/a \in [0, 1]$. The R_{2n}^0 cannot be interpreted directly in physical terms, unlike the velocity profiles $v^{(\ell)}$ in Eq. (6), in which ℓ has the interpretation of a smoothness parameter for the transition from the nonzero values on the piston ($\sigma < a$) to the value zero outside the piston ($\sigma > a$). Rather, their significance for loudspeaker analysis stems from the following facts.

- They are very efficient and convenient in representing a general velocity profile v. This is due to the orthogonality property

$$\int_0^1 R_{2n_1}^0(\rho)R_{2n_2}^0(\rho)\,\rho\,d\rho = \begin{cases}\dfrac{1}{2(2n_1+1)}, & n_1 = n_2\\ 0, & n_1 \neq n_2\end{cases} \quad (9)$$

as well as the fact that many velocity profiles considered in loudspeaker analysis can be represented as a Zernike series. In [1, app. A] a number of cases are listed, such as the expansions for the velocity profiles in Eqs. (6) and (7).

Table 1. Zernike polynomials.

n	$R_{2n}^0(\sigma/a)$
0	1
1	$2(\sigma/a)^2 - 1$
2	$6(\sigma/a)^4 - 6(\sigma/a)^2 + 1$
3	$20(\sigma/a)^6 - 30(\sigma/a)^4 + 12(\sigma/a)^2 - 1$

- The Hankel transform of zeroth order of the R_{2n}^0 has a closed form,

$$\int_0^a J_0(u\sigma)R_{2n}^0(\sigma)\sigma\ d\sigma = (-1)^n\frac{a}{u}J_{2n+1}(ua). \quad (10)$$

This formula has been proved in [3] as a special case of a formula expressing the mth-order Hankel transform of Zernike polynomials of azimuthal order m in terms of Bessel functions of the first kind. This formula is very important for the development of explicit analytic results in the spirit of [7]. It gives, for instance, the far-field expression for the pressure due to a single term R_{2n}^0 in the velocity profile, (see Section 3.2 and [1, app. B]).

3 ON-AXIS AND FAR-FIELD EXPRESSIONS

The velocity profile $v(\sigma)$ considered in this section (normal component) vanishes outside the disk $\sigma \le a$ and has been developed into a Zernike series as in Eq. (4) with coefficients u_n given in accordance with Eq. (5), or explicitly as in the cases discussed earlier.

3.1 On-Axis Expression

For an on-axis point $\boldsymbol{r} = (0, 0, r)$ with $r \ge 0$ the following formula holds [1]:

$$p(\boldsymbol{r}) = \frac{1}{2}V_s\,\rho_0 c(ka)^2\sum_{n=0}^{\infty}\gamma_n(k, r)u_n \quad (11)$$

in which

$$\gamma_n(k, r) = (-1)^n j_n(kr_-)h_n^{(2)}(kr_+), \qquad r_\pm = \frac{1}{2}(\sqrt{r^2+a^2} \pm r). \quad (12)$$

The $r_\pm$ in Eq. (12) satisfy

$$0 \le r_- \le \frac{1}{2}a \le r_+, \qquad r_+r_- = \frac{1}{4}a^2, \qquad r_+ + r_- = \sqrt{r^2+a^2}. \quad (13)$$

The j_n and $h_n^{(2)} = j_n - \mathrm{i}y_n$ are the spherical Bessel and Hankel functions, respectively, of order $n = 0, 1, \ldots$ (see [13, sec. 10.1]). In particular, $j_0(z) = (\sin z)/z$ and $h_0^{(2)}(z) = (\mathrm{i}e^{-\mathrm{i}z})/z$.

Fig. 4 shows a plot of $|\gamma_{\ell=n=0}(k, r)|$ as a function of r/a (rigid piston) and of $|\gamma_n(k, r)|$ for $n = 1, 2, 3$. Some comments on these plots are presented at the end of this subsection.

The result in Eqs. (11) and (12) comprises the known result [8, sec. 8.31a,b] for the rigid piston with $p(\boldsymbol{r})$, $\boldsymbol{r} = (0, 0, r)$, given by

$$p(\boldsymbol{r}) = \frac{1}{2}V_s\rho_0 c(ka)^2\frac{\sin kr_-}{kr_-}\frac{\mathrm{i}e^{-\mathrm{i}kr_+}}{kr_+} = 2\mathrm{i}\rho_0 cV_s e^{-\frac{1}{2}\mathrm{i}k[(r^2+a^2)^{\frac{1}{2}}+r]}\sin\frac{1}{2}k[(r^2+a^2)^{\frac{1}{2}}-r)] \quad (14)$$

and it generalizes immediately to the case of the simply supported radiator ($\ell = 1$) and the clamped radiators.

In Fig. 5 the rigid piston ($\ell = 0$), the simply supported radiator ($\ell = 1$), and the first two clamped radiators ($\ell = 2, 3$) are considered ($|p(\boldsymbol{r})|$, normalized as a function of r/a).

The following comments concern the behavior of the terms γ_n in Eq. (12). From Eqs. (12) and (13) it follows that

$$r_- \approx \frac{1}{2}(a-r) \approx \frac{1}{2}a \approx \frac{1}{2}(a+r) \approx r_+, \qquad r \ll a. \quad (15)$$

Therefore when ka is large and $r \to 0$ (with n not large), it follows from the results in [13, sec. 10.1] that

$$|\gamma_n(k,r)| \approx \frac{\left|\cos\frac{1}{2}k(a-r)\right|}{\frac{1}{4}k^2a^2} \quad (16)$$

confirming the presence of zeros and the largely n-independent envelope of the curves in Fig. 4 near $r = 0$.

Finally, when $r \gg a$ it follows from Eqs. (12) and (13) that

$$r_- \approx \frac{a^2}{4r}, \qquad r_+ \approx r. \quad (17)$$

Therefore from [13, sec. 10.1],

$$\gamma_n(k,r) \approx \frac{\left(\frac{-\mathrm{i}ka^2}{4r}\right)^n}{1\cdot 3\cdots(2n+1)} \; \frac{\mathrm{e}^{-\mathrm{i}kr_+}}{-\mathrm{i}kr_+} \quad (18)$$

which shows an $O(1/r^{n+1})$ behavior of $\gamma_n(k, r)$ as $n \to \infty$.

3.2 Far-Field Expression

Using the Zernike expansion [Eq. (4)] of $v(\sigma)$ it is shown in [1, app. B] that the following far-field approximation holds: when $\boldsymbol{r} = (r \sin\theta, 0, r\cos\theta)$ and $r \to \infty$,

$$p(\boldsymbol{r}) \approx \mathrm{i}\rho_0 ckV_\mathrm{s}\frac{\mathrm{e}^{-\mathrm{i}kr}}{r}a^2\sum_{n=0}^{\infty}u_n(-1)^n\frac{J_{2n+1}(ka\sin\theta)}{ka\sin\theta}. \quad (19)$$

In the case of a rigid piston it follows that

$$p(\boldsymbol{r}) \approx \mathrm{i}\rho_0 cka^2V_\mathrm{s}\frac{\mathrm{e}^{-\mathrm{i}kr}}{r} \; \frac{J_1(ka\sin\theta)}{ka\sin\theta}. \quad (20)$$

This is the familiar result for the far-field pressure of a rigid piston as can be found in the textbooks, (see, for example, Kinsler et al. [8, eq. (8.35)]). Fig. 6 shows a plot of $\left|\frac{[J_{2n+1}(ka\sin\theta)]}{ka\sin\theta}\right|$, $n = 0, 1, 2, 3$, as a function of $ka \sin\theta$.

For the simply supported radiator, case $\ell = 1$ in Eq. (6), and for the clamped radiators, case $\ell \geq 2$ in Eq. (6), the coefficients u in the Zernike expansion of $v^{(\ell)}$ in Eq. (6) are available [1, app. A], and this gives the far-field approximation of $p(\boldsymbol{r})$ via Eq. (19), see Fig. 7.

Some comments on the behavior of the terms $J_{2n+1}(z)/z$, $z = ka \sin\theta$, as they occur in the series in Eq. (19), are presented now. From the asymptotics of the Bessel functions, as given in [13, eq. 9.3.1], it is seen that in the series in Eq. (19) only those terms contribute significantly for which $2n + 1 \leq \frac{1}{2}\mathrm{e}\,ka\sin\theta$. In particular, when $\theta = 0$, it is only the term with $n = 0$ that is nonvanishing, and this yields

$$p\,[(0,\ 0,\ r)] \approx \frac{1}{2}\mathrm{i}\rho_0 cV_\mathrm{s}\,ka^2\frac{\mathrm{e}^{-\mathrm{i}kr}}{r}, \qquad r \to \infty. \quad (21)$$

This is in agreement with that is found from Eq. (11) when only the term with $n = 0$ is retained and r_+ is replaced by r, r_- is replaced by 0. For small values of ka the terms in the

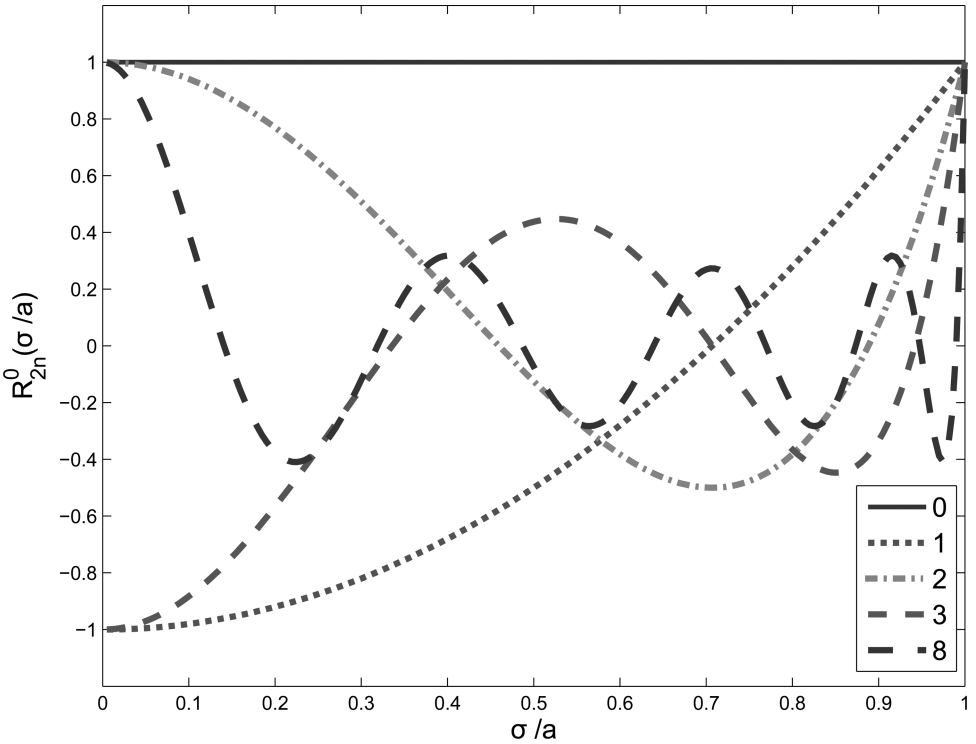

Fig. 3. Zernike terms R^0_{2n} versus σ/a for $n = 0, 1, 2, 3, 8$. Note the increasing number of undulations for increasing n.

series Eq. (19) decay very rapidly with n. For large values of ka, however, a significant number of terms may contribute, especially for angles θ far from 0.

4 POWER OUTPUT AND DIRECTIVITY

The power is defined as the intensity pv^* (where* denotes the complex conjugate) integrated over the plane $z = 0$. Thus because v vanishes outside S,

$$P = \int_S p(\sigma)v^*(\sigma)\,\mathrm{d}S \tag{22}$$

where $p(\sigma) = p[(\sigma\cos\psi, \sigma\sin\psi, 0)]$ is the pressure at an arbitrary point on S. In [2, sec. V] it is shown from Kings's result [15] that

$$P = 2\pi\mathrm{i}\rho_0 ck\int_0^\infty \frac{V(u)V^*(u)}{(u^2-k^2)^{1/2}}u\,\mathrm{d}u \tag{23}$$

where

$$V(u) = \int_0^a J_0(u\sigma)\,v\,(\sigma)\,\sigma\,\mathrm{d}\sigma, \qquad u \geq 0 \tag{24}$$

is the Hankel transform of v. This gives rise, via Eqs. (4) and (10), to the integrals

$$\int_0^\infty \frac{J_{2n_1+1}(au)J_{2n_2+1}(au)}{(u^2-k^2)^{1/2}}\,\mathrm{d}u \tag{25}$$

and these have been evaluated in [2, sec. V.B] in the form of a power series in ka.

We next consider the directivity. With the usual approximation arguments in the Rayleigh integral representation of p in Eq. (1) if follows that [$\boldsymbol{r} = (r\cos\psi\sin\theta, r\sin\psi, \sin\theta, r\cos\theta)$]

$$p(\boldsymbol{r}) \approx \mathrm{i}\rho_0 ck\frac{\mathrm{e}^{-\mathrm{i}kr}}{r}V(k\sin\theta). \tag{26}$$

From this there results the directivity

$$D = \frac{4\pi|V(0)|^2}{\int_0^{2\pi}\int_0^{\pi/2}|V(k\sin\theta)|^2\sin\theta\,\mathrm{d}\psi\,\mathrm{d}\theta} = \frac{2|V(0)|^2}{\int_0^{\pi/2}|V(k\sin\theta)|^2\sin\theta\,\mathrm{d}\theta} \tag{27}$$

(see Kinsler et al. [8, sec.8.9]). By Eqs. (2) and (24) it holds that $V(0) = \frac{1}{2}a^2V_s$ and

$$\int_0^{\pi/2}|V(k\sin\theta)|^2\sin\theta\,\mathrm{d}\theta = \frac{1}{2\pi\rho_0 ck^2}\Re\,[P]. \tag{28}$$

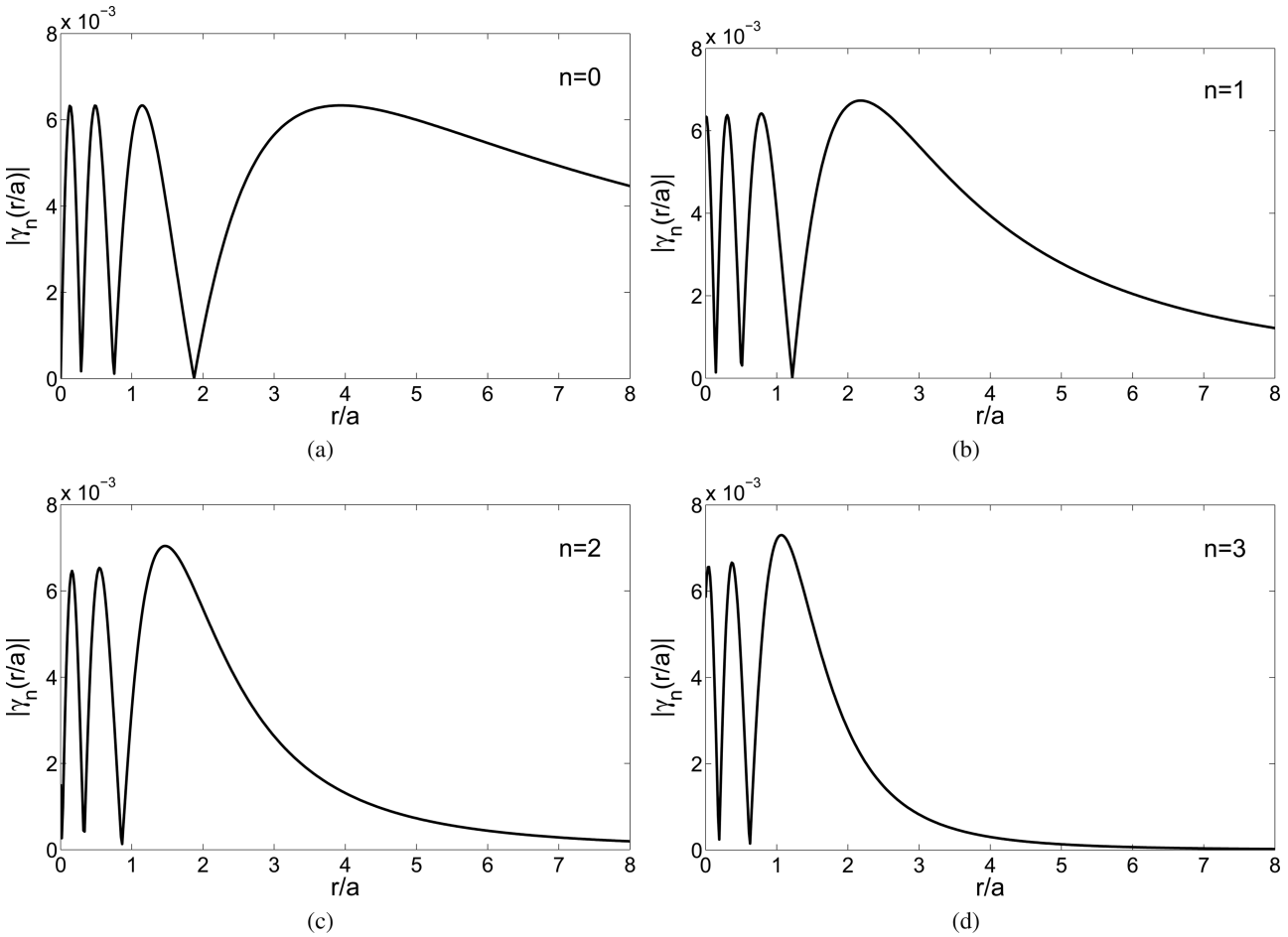

Fig. 4. Product $|j_n(kr_-)h_n^{(2)}(kr_+)|$ from Eq. (12), for $n = 0, \ldots, 3$, versus r/a, where $a/\lambda = 4$ and $a = 0.1$ m, yielding $f = 13.7$ kHz and $ka = 8\pi$. (a) $n = 0$. (b) $n = 1$. (c) $n = 2$. (d) $n = 3$.

Consider the case where $ka \to 0$. In [2] it is derived that $\Re[P] \approx \frac{1}{2}\pi\rho_0 c V_s^2 a^2 (ka)^2$. Therefore as $ka \to 0$,

$$D \approx \frac{2(\frac{1}{2}a^2 V_s)^2}{1/(2\pi\rho_0 c k^2)\frac{1}{2}\pi\rho_0 c V_s^2 a^2 (ka)^2} = 2 \tag{29}$$

or 3 dB. This limiting value of 2 for D is also found in the case of a rigid piston [8] or a hemispherical source on an infinite baffle.

Next consider the case where $ka \to \infty$. It is shown in [2, sec. V.D] that

$$D \approx \frac{2(\frac{1}{2}a^2 V_s)^2}{1/(2\pi\rho_0 c k^2) 2\pi\rho_0 c a^2 \int_0^1 |v(a\rho)|^2 \rho \, d\rho} = \frac{\frac{1}{2}(ka)^2 V_s^2}{\int_0^1 |v(a\rho)|^2 \rho \, d\rho} = C_v (ka)^2 \tag{30}$$

in which C_v is the ratio of the square of the modulus of the average velocity and the average of the square of the modulus of the velocity (averages over S). In the case where $v = v^{(\ell)}$, the last member of Eq. (30) is given by $(2\ell + 1)(\ell + 1)^{-1} (ka)^2$. This result is given in Kinsler et al. [8, end of subsec. 8.9] for the case $\ell = 0$.

5 ESTIMATING VELOCITY PROFILES FROM ON-AXIS RADIATION DATA FOR FAR-FIELD LOUDSPEAKER ASSESSMENT

5.1 Estimating Velocity Profiles from On-Axis Radiation

The on-axis expression [Eqs. (11) and (12)] for the pressure can, in reverse direction, be used [1] to estimate the velocity profile on the disk from (measured) on-axis data via its expansion coefficients u_n. This can be effected by adopting a matching approach in which the coefficients u_n in the "theoretical" expression [Eqs. (11) and (12)] are determined so as to optimize the match with measured data at $M + 1$ points. Thus for the pressure $p_m = p[(0, 0, r_m)]$ due to the velocity profile $v(\sigma) = V_s \Sigma_{n=0}^N u_n R_{2n}^0(\sigma/a)$ one has the expression

$$p_m = \tfrac{1}{2}\rho_0 c V_s (ka)^2 \sum_{n=0}^{N} (-1)^n j_n(kr_{m,-}) h_n^{(2)}(kr_{m,+}) \, u_n \tag{31}$$

where $r_m \geq 0$ and

$$r_{m,\pm} = \frac{1}{2}\left(\sqrt{r_m^2 + a^2} \pm r_m\right), \qquad m = 0, 1, \ldots, M. \tag{32}$$

With

$$A = (A_{mn})_{\substack{m=0,1,\ldots,M,\\ n=0,1,\ldots,N}}$$

$$A_{mn} = \tfrac{1}{2}\rho_0 c V_s (ka)^2 j_n(kr_{m,-}) h_n^{(2)}(kr_{m,+}) \tag{33}$$

$$\boldsymbol{p} = [p_0, \ldots, p_M]^{\mathrm{T}}, \qquad \boldsymbol{u} = [u_0, \ldots, u_N]^{\mathrm{T}} \tag{34}$$

the relation between on-axis pressures p_m and coefficients u_n can be concisely written as

$$A\boldsymbol{u} = \boldsymbol{p}. \tag{35}$$

Now given a (noisy) on-axis data vector $\boldsymbol{p}$ one can estimate the coefficient vector $\boldsymbol{u}$ by adopting a least-mean-squares approach for the error $A\boldsymbol{u} - \boldsymbol{p}$. This will be illustrated next by a simulated experiment and, subsequently, by a real experiment. In the simulated experiment we assume a loudspeaker with a Gaussian velocity profile ($\alpha = 2$), as shown in Fig. 8(a), curve v_G (–·–). This profile is approximated using three Zernike coefficients ($u_0 = 0.4323$, $u_1 = -0.4060$, $u_2 = 0.1316$), and this leads to the velocity profile v_a (——) in Fig. 8(a). It can be seen from Fig. 8(a) that including three Zernike terms provides a fair approximation

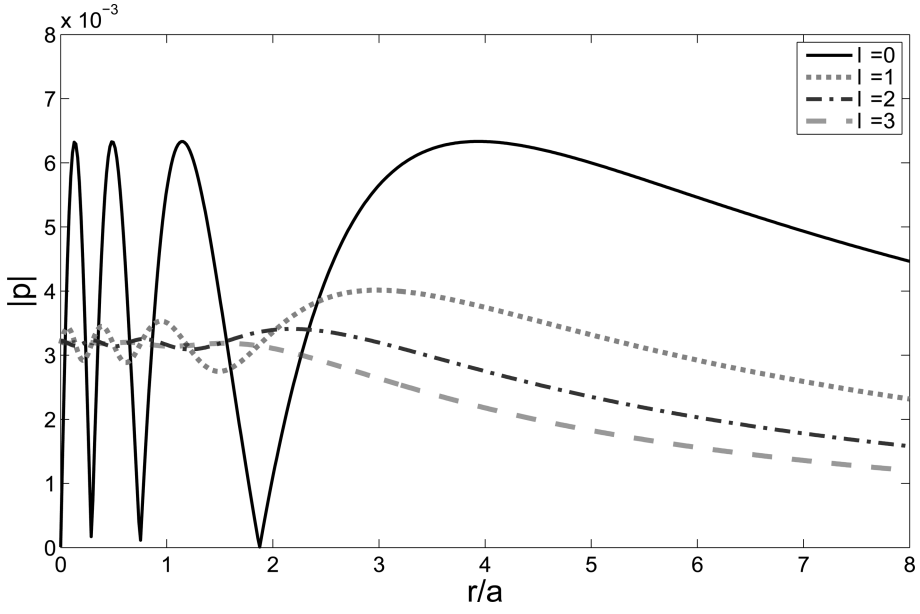

Fig. 5. Normalized $|p|$ versus r/a for rigid piston ($\ell = 0$) (——); simply supported radiator ($\ell = 1$) (· · ·); and first two clamped radiators ($\ell = 2, 3$) (–·–, – – –) using Eq. (11). Here $a/\lambda = 4$ and $ka = 8\pi$. Normalization is equal to $(\ell + 1)/2 \, \rho_0 c V_s (ka)^2$. The factor $\ell + 1$ allows for an easier comparison of the curves.

(3×10^{-2} absolute accuracy on the whole range). Using the three coefficients of the approximated velocity profile, the sound pressure was calculated by applying Eq. (11) and plotted in Fig. 8(b) as p_{calc} (——). Then random white noise was added to p_{calc}, shown as p+noise in Fig. 8(b) (. . . .) Subsequently the inversion procedure was followed by using the noisy pressure data vector $\boldsymbol{p}$ to estimate the coefficient vector $\boldsymbol{u}$ by adopting a least-mean-squares approach for the error $A\boldsymbol{u} - \boldsymbol{p}$ [see Eq. (35)]. Using the recovered three Zernike coefficients the velocity profile and pressure data were calculated and plotted in Fig. 8(a) and (b) (heavy dotted curves). It appears that the

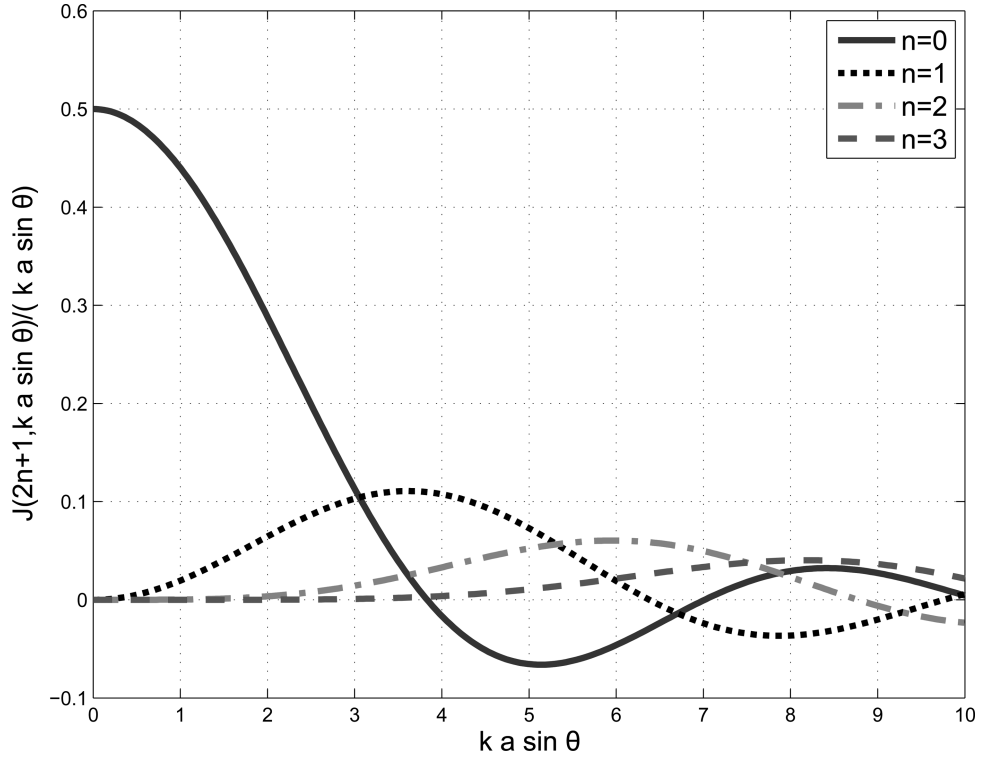

Fig. 6. $\left|\frac{[J_{2n+1}(ka\sin\theta)]}{ka\sin\theta}\right|$ versus ka sin θ.

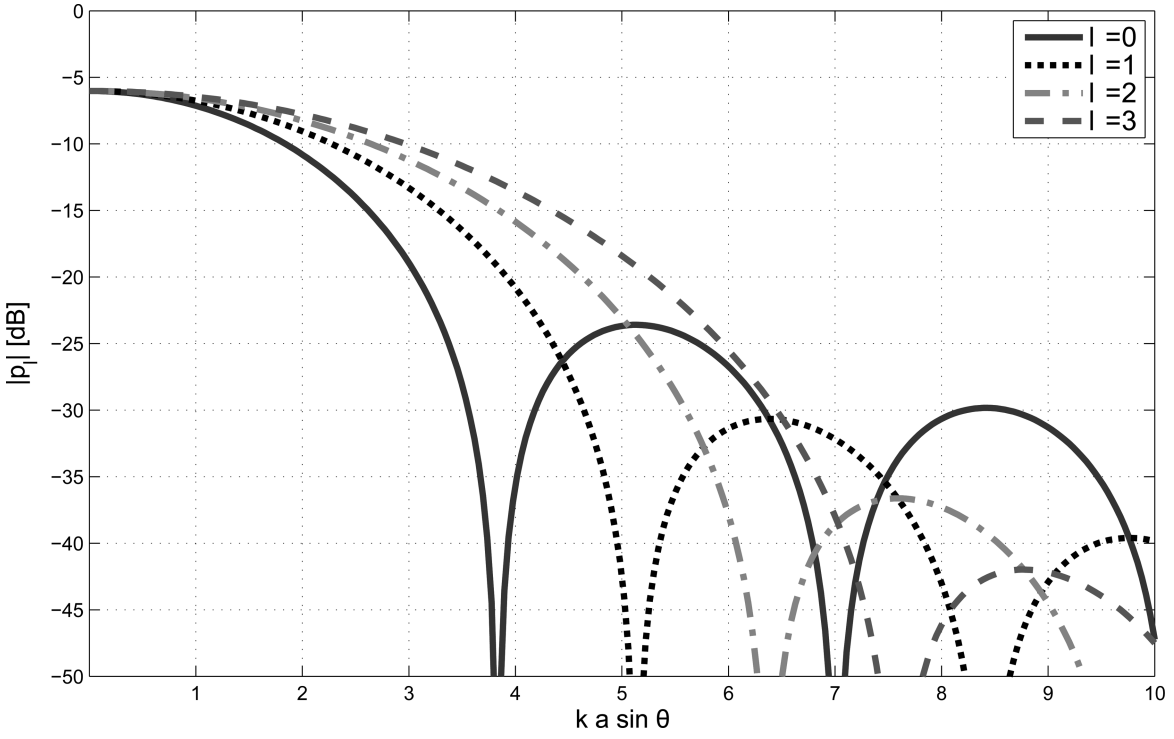

Fig. 7. Normalized |p| versus ka sin θ, using the Zernike expansion of $v^{(\ell)}$ and Eq. (19).

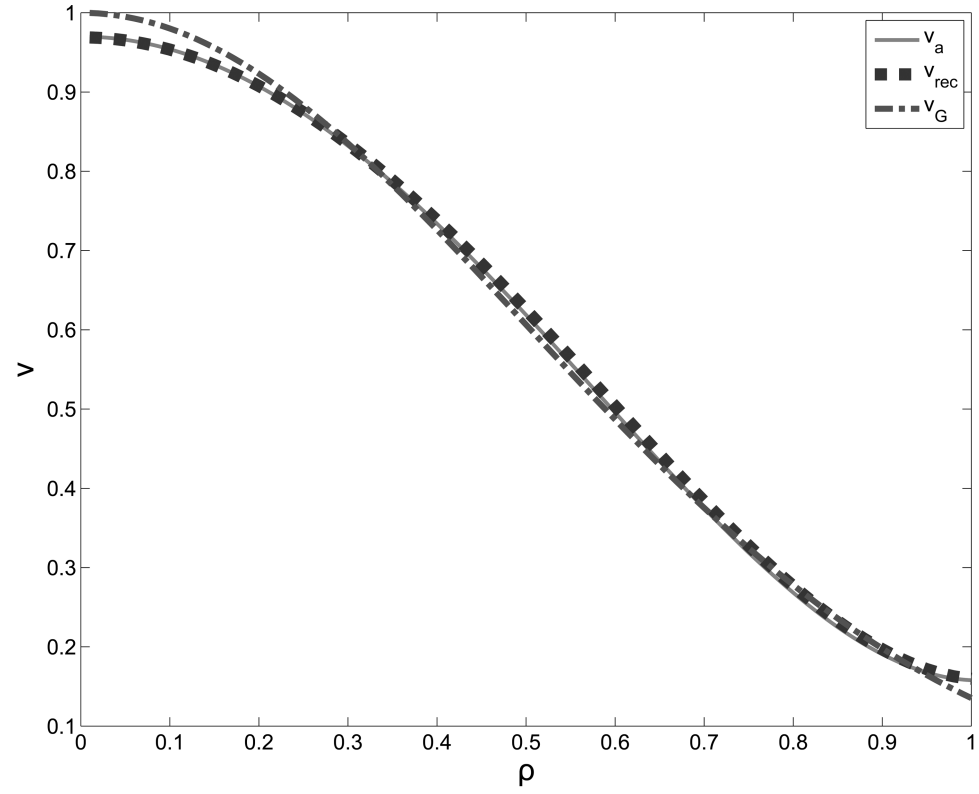

(a)

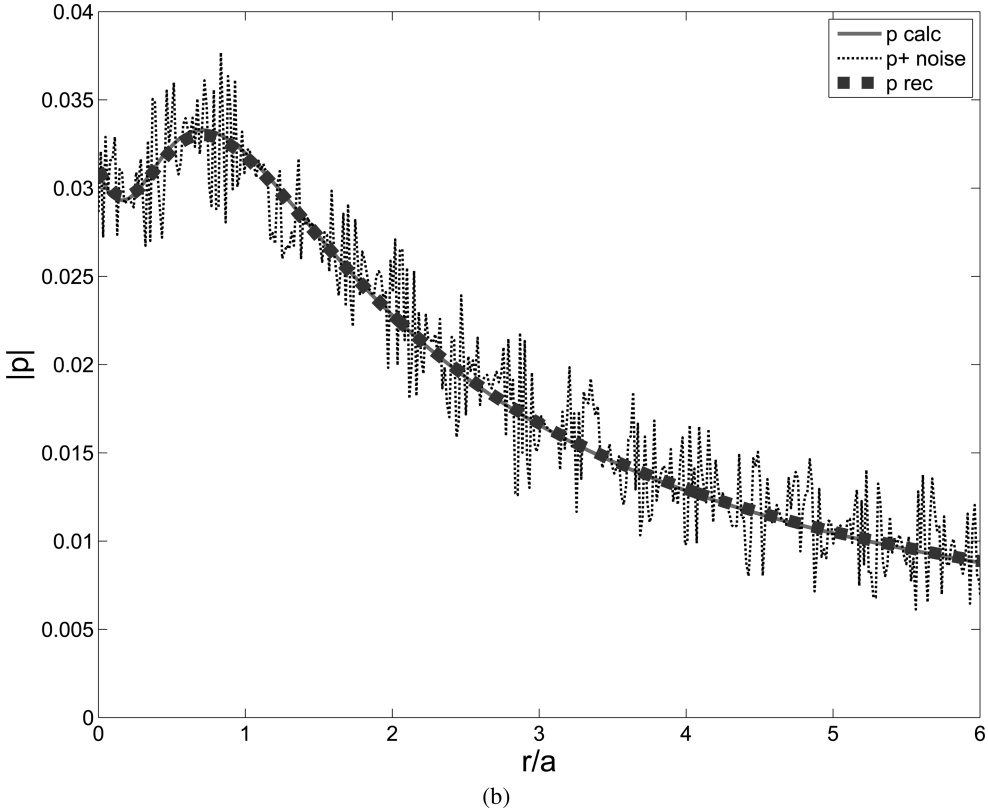

(b)

Fig. 8. Simulated experiment. (a) Gaussian velocity profile ($\alpha = 2$) v_G versus ρ (–·–); approximated velocity profile v_a Zernike series expansion of [1, app. A] truncated at $n = 2$ (——); and velocity profile v_{rec} recovered from noisy pressure data (· · ·). (b) Sound pressure using Eq. (11) and $ka = 8$ (p_{calc}, ——); pressure with added noise (p+noise, · · ·); and recovered pressure data (p_{rec}, ■■■). Note, solid curve is almost coincident with p_{rec} curve, but is visible between dots.

inversion procedure is rather robust against noise since the calculated and recovered pressure curves in Fig. 8(b) are almost coincident.

For the second experiment we measured a loudspeaker (Vifa MG10SD09-08, a = 32 mm) in an IEC baffle [16], with the microphone placed at various positions on a straight line at ten near-field points at zero degree observation angle ($\boldsymbol{r}_m$ = 0.00, 0.01, 0.02, 0.03, 0.04, 0.05, 0.07, 0.10, 0.13, 0.19 m), and finally the bottom curve for the far field at 1-m distance. The sound pressure level plotted in Fig. 9 clearly shows that the near field differs form the far field, in particular at higher frequencies. The lower curve is somewhat noisy because the amplification of the microphone amplifier was kept the same for all measurements.

For a particular frequency of 13.72 kHz (ka = 8.0423) the magnitude of the sound pressure is plotted in Fig. 10 (p_{meas}). Using the same procedure as described for the first simulation, the inverse process was followed by using the ten measured near-field pressure data points to estimate the coefficient vector $\boldsymbol{u}$. Using four Zernike coefficients the pressure data were recovered and plotted in Fig. 10 (p_{rec}). It appears that the two curves show good resemblance to each other and that only four coefficients are needed to provide a very good description of the near field at rather high frequencies (13.72 kHz). Furthermore it appears that using these four coefficients, the calculated sound pressure level at 1-m distance yields −42 dB. The measured value at that far-field point is −44 dB. These values match rather closely, even though the cone no longer vibrates fully circular, symmetrically at the frequency of 13.72 kHz used because of break-up behavior. This match provides a proof of principle as the far-field measurement point was not used to determine the Zernike coefficients (See also Section 5.2).

In the experiments just described no particular effort was made in forming and handling the linear systems so as to have small condition numbers. The condition number, the ratio of the largest and smallest nonzero singular values of matrix A in Eq. (33), equals 50 in the case of the loudspeaker experiment leading to Fig. 10. In practical cases the number of required Zernike coefficients will be less than, say, six. This will not cause numerical difficulties. Furthermore such a modest number of coefficients already parameterizes a large set of velocity profiles.

5.2 Far-Field Assessment from On-Axis Measurements

In Keele [9] a method is described to assess low-frequency loudspeaker performance in the on-axis far field from an on-axis near-field measurement. In the case of the rigid piston, the on-axis pressure $p(\boldsymbol{r}) = p[(0, 0, r)]$ is given by Eq. (14). Now assume $ka \ll 1$. When $r \ll a$ it holds that

$$\sin\left[\frac{1}{2}k\left(\sqrt{r^2+a^2}-r\right)\right] \approx \sin\left(\frac{1}{2}ka\right) \approx \frac{1}{2}ka \qquad (36)$$

and when $r \gg a$, it holds that

$$\sin\left[\frac{1}{2}k\left(\sqrt{r^2+a^2}-r\right)\right] \approx \sin\left(\frac{ka^2}{4r}\right) \approx \frac{ka^2}{4r}. \qquad (37)$$

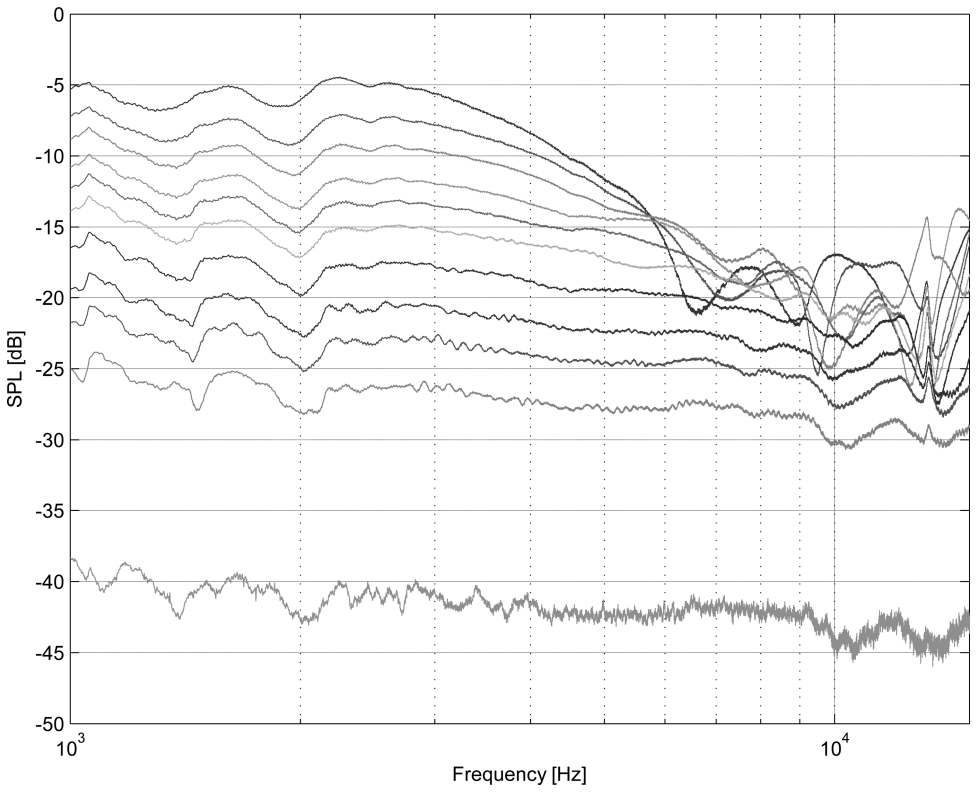

Fig. 9. Measured SPL (with arbitrary reference level) for loudspeaker (Vifa MG10SD09-08, a = 32 mm) in an IEC baffle [16] at 10 near-field positions from upper curve (0.00, 0.01, 0.02, 0.03, 0.04, 0.05, 0.07, 0.10, 0.13, 0.19 m). Bottom curve is for far field at 1-m distance.

Therefore the ratio of the moduli of near-field and far-field on-axis pressure is given by $2r/a$. This is the basis of Keele's method. It allows far-field loudspeaker assessment without having to use an anechoic room.

With the inversion procedure to estimate velocity profiles from on-axis data (which are taken in the relative near field), as described in Section 5.1 together with the forward calculation scheme for the far field as described in Section 3.2, it is now possible to generalize Keele's scheme. This is illustrated by comparing the far-field responses pertaining to the two sets of Zernike coefficients occurring in the Gaussian simulated experiment (see Fig. 8). Using Eq. (19) the normalized far-field pressure is plotted in Fig. 11 as p_{calc} and p_{rec} ($\alpha = 2$, $ka = 8$), where the normalization is such that the factor in front of the series at the right-hand side of Eq. (19) equals unity. It appears that the two curves are very similar. This confirms that the u_n obtained from the noisy near-field

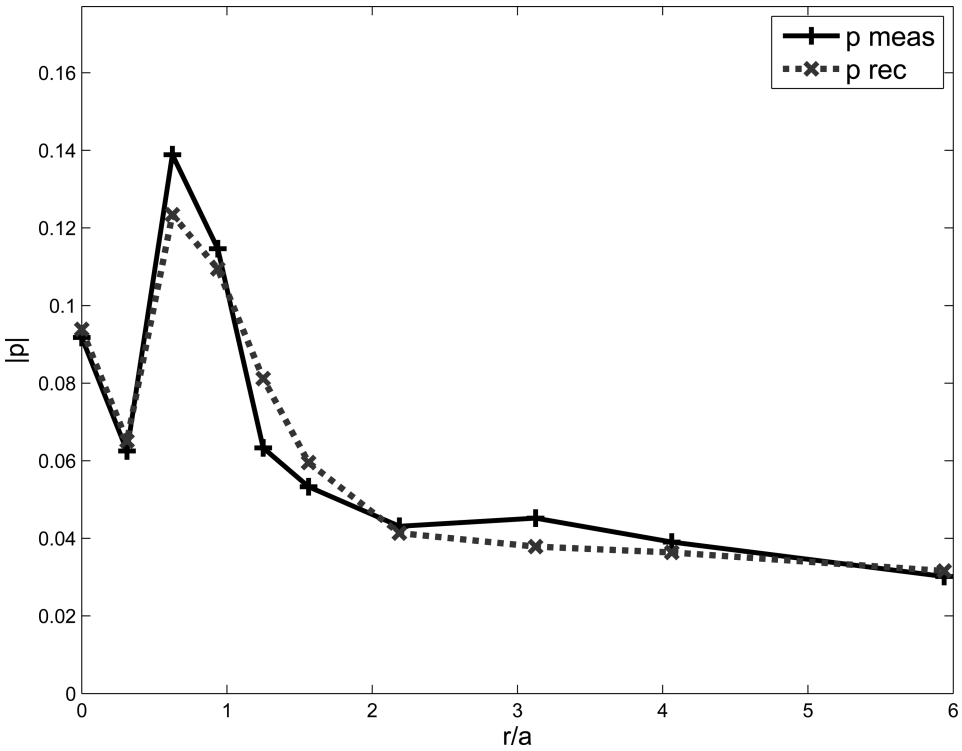

Fig. 10. Sound pressure radiated [a.u.] by loudspeaker, measured at 13.72 kHz ($ka = 8.0423$, p_{meas}, ——) and recovered pressure data (p_{rec}, ■■■) versus r/a.

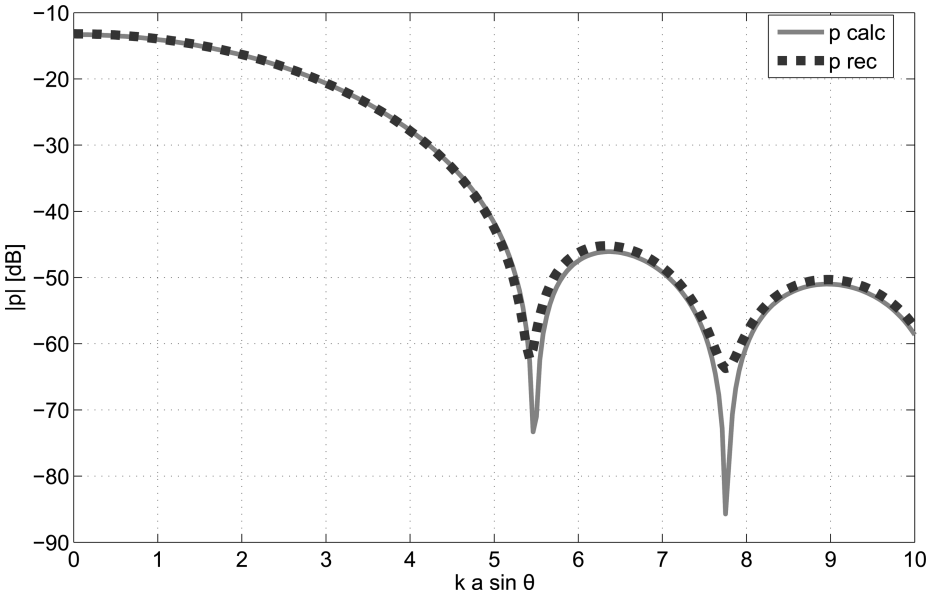

Fig. 11. Simulated experiment for Gaussian radiator ($\alpha = 2$). Normalized sound pressure in far field using Eq. (19) and $ka = 8$ (p_{calc}, ——) and recovered normalized far-field pressure data (p_{rec}, ■■■).

measured pressure data yield a good estimate of the far-field spatial pressure response.

6 DISCUSSION AND OUTLOOK

This paper has considered a method to perform forward and inverse sound pressure computations for circular radiators with a nonuniform velocity profile. However, it must be stated that not all drivers move in a circularly symmetric fashion. Shallow cones have significant circumferential modes. For example, automotive loudspeakers and transducers without spider (headphones and microspeakers) suffer from rocking modes. This needs further research.

In the forward problem the velocity profile is assumed to be known and the on-axis and far-field sound pressures are expressed analytically in terms of Zernike expansion coefficients of the velocity profile and (spherical) Bessel (and Hankel) functions. In the inverse problem the velocity profile is unknown and is estimated in terms of Zernike expansion coefficients from on-axis pressure data by adopting a matching approach based on the analytic result for the on-axis pressure. Well-behaved velocity profiles are already adequately represented by only a few terms of their Zernike expansion. Therefore the Zernike series approach is more convenient for both the forward problems and the inverse problem than, for instance, an approach based on expansions involving the family of rigid, simply supported, and clamped radiators. The forward and inverse method is proposed for use in the assessment of the far field of a loudspeaker without the need for an anechoic room. Here the Zernike coefficients of the velocity profile are estimated from the on-axis (relatively near-field) data, and these coefficients are used in the forward scheme to compute the far field. This assessment procedure has not been worked out fully in the present paper because of a variety of practical issues that need to be addressed. Among these practical issues are

- Choice of on-axis measurement points
- Condition of linear systems that arise
- Influence of ka
- Influence of noise
- Influence of misalignment of the measurement points
- Influence of inclination of the measurement axis
- Incorrect setting of the radiator radius
- Accuracy of the identified velocity profile and role of this intermediate result.

Various combinations of these issues should also be considered. It can already be said that in practice the number of retrieved Zernike coefficients will be on the order of five. The real number will depend on the condition number of the matrix A in Eq. (35). The authors intend to work on the method for loudspeaker assessment with attention to the points mentioned.

In this paper the theory has been developed for flat radiators. However, the basic result for the on-axis pressure as a series expansion, in terms of Zernike coefficients and spherical Bessel and Hankel functions, has been generalized to the case of dome-shaped radiators [1]. Furthermore the theory is adapted to spherical loudspeaker cabinets, where the loudspeaker is modeled as a moving cap on the sphere [11]. It is therefore to be expected that both the forward and the inverse methods can also be generalized to the case of dome-shaped radiators. The authors intend to develop the method on both a theoretical and a practical level for dome-shaped radiators as well.

7 CONCLUSIONS

Zernike polynomials are an efficient and robust method to describe velocity profiles of resilient sound radiators. A wide variety of velocity profiles, including the rigid piston, the simply supported radiator, clamped radiators, Gaussian radiators, as well as real loudspeaker drivers, can be approximated accurately using only a few terms of their Zernike expansions. This method enables one to solve both the forward and the inverse problem. With the forward method the on-axis and the far-field off-axis sound pressures are calculated for a given velocity profile. With the inverse method the actual velocity profile of the radiator is calculated using (measured) on-axis sound pressure data. This computed velocity profile allows extrapolation to far-field loudspeaker pressure data, including off-axis behavior, without the use of anechoic rooms.

8 REFERENCES

[1] R. M. Aarts and A. J. E. M. Janssen, "On-Axis and Far-Field Sound Radiation from Resilient Flat and Dome-Shaped Radiators," *J. Acoust. Soc. Am.*, vol. 125, pp. 1444–1455 (2009 Mar.).

[2] R. M. Aarts and A. J. E. M. Janssen, "Sound Radiation Quantities Arising from a Resilient Circular Radiator," *J. Acoust. Soc. Am.*, vol. 126, pp. 1776–1787 (2009 Oct.).

[3] B. R. A. Nijboer, "The Diffraction Theory of Aberrations," Ph.D. dissertation, University of Groningen, Groningen, The Netherlands (1942).

[4] F. Zernike and B. R. A. Nijboer, "The Theory of Optical Images" (in French), *Revue d'Optique* (Paris), p. 227 (1949).

[5] M. Born and E. Wolf, *Principles of Optics*, 7th ed. (Cambridge University Press, Cambridge, MA, 2002), chap. 9.

[6] J. J. M. Braat, S. van Haver, A. J. E. M. Janssen, and P. Dirksen, "Assessment of Optical Systems by Means of Point-Spread Functions," in *Progress in Optics*, vol. 51, E. Wolf, Ed. (Elsevier, Amsterdam, The Netherlands, 2008), chap. 6.

[7] M. Greenspan, "Piston Radiator: Some Extensions of the Theory," *J. Acoust. Soc. Am.*, vol. 65, pp. 608–621, (1979).

[8] L. E. Kinsler, A. R. Frey, A. B. Coppens, and J. V. Sanders, *Fundamentals of Acoustics* (Wiley, New York, 1982).

[9] D. B. Keele, Jr., "Low-Frequency Loudspeaker Assessment by Nearfield Sound-Pressure Measurement," *J. Audio Eng. Soc.*, vol. 22, pp. 154–162 (1974 Apr.).

[10] J. W. S. Rayleigh, *The Theory of Sound*, vol. 2 (1896) (Reprinted, Dover, New York, 1945).

[11] R. M. Aarts and A. J. E. M. Janssen, "Modeling a Loudspeaker as a Resilient Spherical Cap on a Rigid Sphere," to be presented at the 128th Convention of the Audio Engineering Society, London, UK, 2010 May 20–23.

[12] F. J. M. Frankort, "Vibration and Sound Radiation of Loudspeaker Cones," Ph.D. dissertation, Delft University of Technology, Delft, The Netherlands (1975).

[13] M. Abramowitz and I. A. Stegun, *Handbook of Mathematical Functions* (Dover, New York, 1972).

[14] H. Stenzel, "On the Acoustical Radiation of Membranes" (in German), *Ann. Physik*, vol. 7, pp. 947–982 (1930).

[15] L. V. King, "On the Acoustic Radiation Field of the Piezo-Electric Oscillator and the Effect of Viscosity on Transmission," *Can. J. Res.*, vol. 11, pp. 135–155 (1934).

[16] IEC 60268-5, "Sound System Equipment—Part 5: Loudspeakers," International Electrotechnical Commission (IEC), Geneva, Switzerland (2007).

THE AUTHORS

R. M. Aarts

A. J. E. M. Janssen

Ronald M. Aarts was born in Amsterdam, The Netherlands, in 1956. He received a B.Sc. degree in electrical engineering in 1977, and a Ph.D. degree in physics from the Delft University of Technology, Delft, The Netherlands, in 1995.

He joined the optics group at Philips Research Laboratories, Eindhoven, The Netherlands, in 1977. There he initially investigated servos and signal processing for use in both Video Long Play players and Compact Disc Players. In 1984 he joined the acoustics group and worked on the development of CAD tools and signal processing for loudspeaker systems. In 1994 he became a member of the digital signal processing (DSP) group and has led research projects on the improvement of sound reproduction by exploiting DSP and psychoacoustical phenomena. In 2003 he became a research fellow and extended his interests in engineering to medicine and biology. He is a part-time full professor at the Eindhoven University of Technology.

Dr. Aarts has published a large number of papers and reports and holds over one hundred granted and pending U.S. patents in his field. He has served on a number of organizing committees and as chair for various international conventions. He is a Fellow of the IEEE, a Fellow and past governor of the AES, and a member of the NAG (Dutch Acoustical Society), the Acoustical Society of America, and the VvBBMT (Dutch Society for Biophysics and Biomedical Engineering).

●

Augustus J. E. M. Janssen received engineering and Ph.D. degrees in mathematics from the Eindhoven University of Technology, Eindhoven, The Netherlands, in 1976 and 1979, respectively.

From 1979 to 1981 he was a Bateman Research Instructor in the Mathematics Department of the California Institute of Technology, Pasadena. From 1981 until recently he worked with Philips Research Laboratories, Eindhoven, where his principal responsibility was to provide high-level mathematical service and consultancy in mathematical analysis. He is currently an independent consultant in mathematical analysis.

In 2003 Dr. Janssen was elected Fellow of the IEEE. He has published over 150 papers in the fields of Fourier analysis, signal analysis, time–frequency analysis, electron microscopy, optical diffraction theory, and queuing theory, and his current interests include the application of techniques from the theory of optical aberrations to the characterization of acoustical radiators.